Measured radiation patterns of the scale model dipole tool

Rongrong Lu, Rama Rao, Nafi Toksöz
Earth Resources Laboratory
Department of Earth, Atmospheric and Planetary Sciences
Massachusetts Institute of Technology
Cambridge, MA 02139

Abstract

The sound field of finite dipole acoustic transducers in a steel tool was investigated and their horizontal by measuring their vertical radiation patterns in water at two different frequencies. Measurements were also made with the tool in scale models representative of sonic logging conditions in the field. A Lucite borehole model was used to represent a soft formation and an Austin Chalk borehole model was used to represent a hard formation.

The presence of the tool as a finite baffle for the transducer, introduces differences between the vertical and horizontal radiation patterns. In contrast to the vertical pattern, the horizontal radiation pattern has a narrower main lobe with relatively larger side lobes. The angular location of the side lobes as seen in the water measurements, do not change much in the borehole.

1. Introduction

Radiation pattern of the transducers in tool is very important for sonic logging and imaging. The radiation pattern of the acoustic waves from an ideal point source and baffled plane piston source have been well-studied by many authors (D'hooge, 1997; Boisvert, 2002). The radiation pattern from relatively complex sources such as a cylindrical source of finite length was also studied (Heelan, 1953; White, 1960). Furthermore, the radiation pattern of seismic sources in open and cased boreholes has been investigated in several important papers (Lee and Balch, 1982; Winbow, 1991; Peng, 1993). To our knowledge, the radiation of a finite sized transducer in a curved, finite baffle, representative of a source in a logging tool, has not been studied in detail. In practice, many important borehole applications, such as near-borehole imaging and geo-steering could benefit from a better understanding of this radiation pattern.

In this paper, the radiation pattern of a scale model dipole tool is studied in detail. Experiments are performed with the tool in water and in borehole models for different source-receiver configurations and frequency bands. Simple analytical models are proposed to explain the experimental results.

The results of these initial experiments need to be interpreted qualitatively to a large extent, as transducers could not be scaled exactly from the field tools. The transducers are larger than those in a real tool for a given tool size, and hence display effects like larger side lobes, compared to full scaled tools

2. Experimental Setup

2.1 Dipole transducer and the tool

The dipole source is made of two PZT disks of 6mm in diameter with the same polarization, as shown in Figure 1. Two PZT crystal plates vibrating in piston mode are glued with conducting epoxy. In the figure, arrows indicate the polarization of crystals and "+" "-" indicate the electrodes.

The electrodes of the two PZT disks are connected in parallel. When a direct voltage with a polarity opposite to the polarization direction of PZT disk is applied to the electrode, the disk contracts. For the opposite case, the disk extends. Therefore, when the electric field is applied, one disk expends while the other contracts, which behaves as a pure dipole source.

2.2 Setup for measurement in water

Figure 2 shows the flow chart of all the experiments. The signal generated by a waveform generator is feed to the source in the tool. After transmitting through the medium, such as water, Lucite and Austin Chalk, the acoustic wave is received by the hydrophone or P-wave receiver. The received signal is amplified and acquired by the digital oscilloscope and then transferred into the computer in the end.

Four different measurement configurations are shown in Figure 3. Generally, the tool is secured on an axis of a rotation motor, and the receiver, a broadband hydrophone (ITC-1089C), is secured on another step motor at the same height.

The first measurement (Figure 3.a) is to measure the sound pressure on the axis of the transducer as a function of distance. In this measurement, the source transducer is fixed and excited by a single-cycle sinusoidal signal. The hydrophone moves along the transducer axis, and the received waves are recorded every 6mm. The frequency for the burst signal is adjustable. To obtain maximum amplitude, the waveforms are recorded at 250KHz, which is the center frequency of the transducer.

The horizontal radiation is measured in the water tank by rotating the tool around the *y*-axis and keeping the hydrophone fixed at a given distance, as shown in Figure 3.b.

The vertical radiation pattern is measured through two methods. In the first approach, the tool is horizontally oriented under the rotation motor on the same plane as the receiver and rotated around the *y*-axis, as shown in Figure 3.c. The second approach is compared to the measurement in borehole. In this method, the tool is again fixed under the motor, and the receiver, which is 10cm away from the tool, is moved vertically along the *y*-axis, as shown in Figure 3.d.

2.3 Setup for measurement in boreholes

The measurement in the borehole is similar to the measurement in water, as shown in Figure 4. Two scale borehole models are used to measure the radiation pattern. The borehole is filled with water, and the tool can rotate inside the hole to measure the horizontal pattern. The receiver is changed to a P-wave transducer (Panametrics V103), which is attached on the outer surface of the block using Vaseline as the coupling material. The receiver can be moved up and down along the surface to measure the vertical pattern. Two source frequencies (100KHz and 250KHz) are used for each model.

To simulate the soft and hard formations, two borehole models are made of Lucite and Austin

Chalk, respectively. The Lucite model is a cylinder with a hole of 1.9cm in diameter, 10cm away from the outer surface. The Austin Chalk model is a rectangular block with a hole of 1.9cm in diameter, 8.9cm away from the outer surface. The compressional velocity and density of Lucite and Austin Chalk are 2680m/s, 1200kg/m^3 and 3980/s, 2050kg/m^3, respectively.

3. Results and discussion

3.1 Measurement in water

(1) Axial sound pressure

Figure 5.a shows the recorded waveforms in the axial sound pressure measurement and the normalized axial sound pressure amplitudes as a function of distance is shown in Figure 5.b. The solid line is the theoretical numerical calculation of the normalized axial amplitude for a piston source in infinite baffle. The monotonic pressure variation indicates that even at the closest distance, we are in the far field of the transducer.

(2) Horizontal radiation pattern

The horizontal radiation patterns in water are measured at two distances (3cm and 15 cm away from the tool) and at two source frequencies (100KHz and 250KHz), and the results are shown in Figure 7. It must be pointed out that since the same dipole transducer will function both as the source and the receiver, the final radiation pattern for the system is the product of the pattern of source and the pattern of the receiver. All the patterns shown in this paper refer to this composite system radiation pattern, assuming the pattern of the receiver is the same as the pattern of the source.

In Figure 7, for a given distance from the source, as frequency increases (i.e., $\boldsymbol{ka = 2\pi a/\lambda}$ increases), the main lobe width reduces while side lobes get stronger. This trend with increasing ka (increasing from 1 to 3) is also observed in the radiation of a piston source in an infinite baffle. However, all features of the radiation pattern of the transducer operating in a finite curved baffle, the tool, are not adequately predicted by the piston in an infinite baffle model as seen in Figure 6.

At a given frequency, as the source-receiver separation increases, the side lobes get stronger relative to the main lobe. As larger separations, the transducer appears more like a point source, and consequently the radiation pattern tends to get omnidirectional. The side lobes are asymmetrical, due to asymmetries in its mounting.

In Figure 8, the horizontal radiation pattern for the same-sized transducer in a tool with larger diameter is shown. The “backing” provided by tool is now larger (15mm diameter versus 10mm diameter), and hence the main lobe is now wider and the side lobes are weaker, with the larger backing it is tending to look like the vertical radiation pattern (see next section).

Thus, for a given tool size, smaller transducers have smaller side lobes, albeit wider main lobes. This suggests that in real tools, side lobes will likely be smaller than those observed here as the transducers used in these measurements are larger than that specified by scaling.

(3) Vertical radiation pattern

The vertical radiation pattern in water (method 1) is shown in Figure 9. In vertical plane passing through the center of the transducer, the steel tool provides a large, albeit curved baffle for the transducer. Consequently there is a single wide main lobe with very small side lobes. This pattern is more similar to that of a piston in an infinite baffle than the horizontal radiation pattern. The presence of small side lobes is likely due to the transducer being slightly inset from the tool surface. A simple calculation of the "shadow effect" due to this inset was made. As shown in Figure 10, locations where $|\boldsymbol{x}| < \boldsymbol{a}$, "see" the full transducer and are unaffected. But for $|\boldsymbol{x}| > \boldsymbol{a}$, a part of the transducer is shadowed by the tool edge and radiation is only due to the remaining part of the transducer. This calculation (Figure 11) shows that the inset is capable of causing weak side lobes, similar to those observed in measurements.

3.2 Measurement in model boreholes

(1) Horizontal radiation pattern

The horizontal radiation patterns in Lucite and Austin Chalk are shown in Figure 12. The trends with frequency are similar to those observed in the water tank measurements.

Overall the main lobes are wider compared to the water measurements. This is likely due to the formation loading on the transducer imposed by the curved borehole. In the water tank, the transducers can vibrate in piston mode with uniform displacement over the entire transducer face because of the uniform impedance load in all directions. However when operating in a borehole, the transducer edges are closer to the formation compared to the center, which likely tapers the transducer vibration amplitudes towards the edges (Figure 13). For a piston in infinite baffle, tapered amplitudes produces a broadening of the main lobe and an amplification of radiation at 0^o-30^o and 150^o-180^o , the regions where side lobes are commonly located (Figure 14). This is consistent with the borehole measurements in Austin Chalk relative to those in water.

Note also that the lobes are wider in the hard formation compared to the soft formation, likely due to stronger tapering caused by the larger formation impedance. This effect needs to be verified with additional analysis.

(2) Vertical radiation pattern

The measured vertical patterns in boreholes are shown in Figure 15. To make a comparison, results in water using vertical measurement method 2 are shown also. From the results, we can see that the vertical radiation patterns are consistent from water to borehole and from soft formation. We can also observe the main lobe becoming narrower in higher frequency ranges. The jaggedness of the measurements in Austin Chalk is likely due to inhomogeneities in the rock and the irregularities in the borehole.

4. Conclusion

In this paper the radiation patterns of a scale model dipole tool in a borehole model made of Lucite and Austin Chalk boreholes are investigated, and their patterns are compared with the patterns in water.

Based on measurements in water, the vertical radiation is distinctly different from the horizontal. The former has a broad main lobe with very small side lobes while the latter has a narrower main lobe with stronger side lobes. This is due to the difference in the backing effect of the tool in the transducer in the two directions. Side lobes get stronger with increasing frequency, increasing distance from the transducer, and increasing formation impedance. Measurements in water identify the angular location of the side lobes, which don't change much even when the tool is in a borehole. However, the relative magnitudes of main lobes to side lobes and their respective widths are altered, depending on formation type. With further measurements and analysis, it will be possible to predict the transducer operation in a borehole based on water measurements.

Acknowledgements

This work was supported by the Earth Resources Laboratory Founding Members and by the Earth Resources Laboratory Borehole Acoustics and Logging Consortium.

References:

Boisvert J.E., Van Buren A.L., Acoustic radiation impedance of rectangular pistons on prolate spheroids, *J.Acoust.Soc.Am.*, 111(2), 867-874, 2002

Chen S.T., Shear-wave logging with dipole sources, *Geophysics*, *53*, 659-667, 1988.

D'hooge J., Nuyts J., et.al., The calculation of the transient near and far field of a baffled piston using low sampling frequencies, *J.Acoust.Soc.Am.*, 102(1), 78-86, 1997

Heelan, P.A., Radiation from a cylindrical source of finite length, *Geophysics*, *18*, 685-696, 1953

Lee M.W., Balch A.H., Theoretical seismic wave radiation from a fluid filled borehole, *Geophysics*, 47, 1308-1314, 1982

Peng C, Cheng C.H., Toksoz M.N, Cased borehole effects on borehole seismic measurements, *Extended Abstracts, C054, EAEG 55th Ann. Mtng*, 1993

Rama Rao, V.N., Roger, M.T., Toksoz M.N, Source radiation patterns in cased boreholes, *Consortium Reports*, 4-1-37, 1997.

White J.E., Use of reciprocity theorem for computation of low-frequency radiation patterns, *Geophysics*, 25, 613-624, 1960

Winbow G.A., Seismic sources in open and cased boreholes, *Geophysics*, 56, 1040-1050, 1991

Zhu Zhenya, Cheng C.H., Toksoz M.N., Experimental study of the flexural waves in the fractured or cased borehole model, *Consortium Reports*, ,

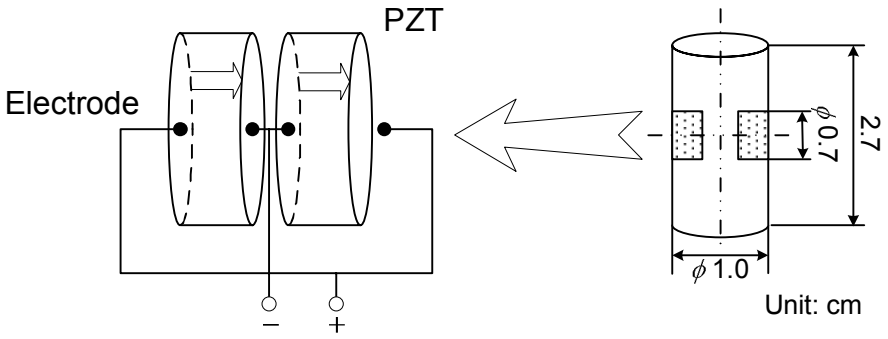

Figure 1 Schematic diagram of a dipole transducer

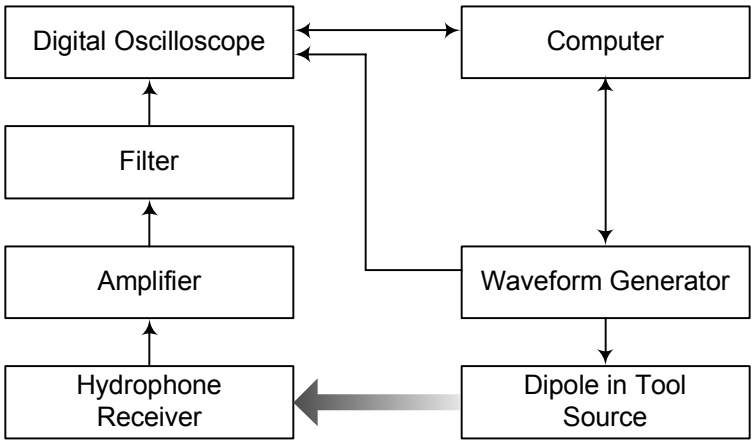

Figure 2 Flow chart of the experiments

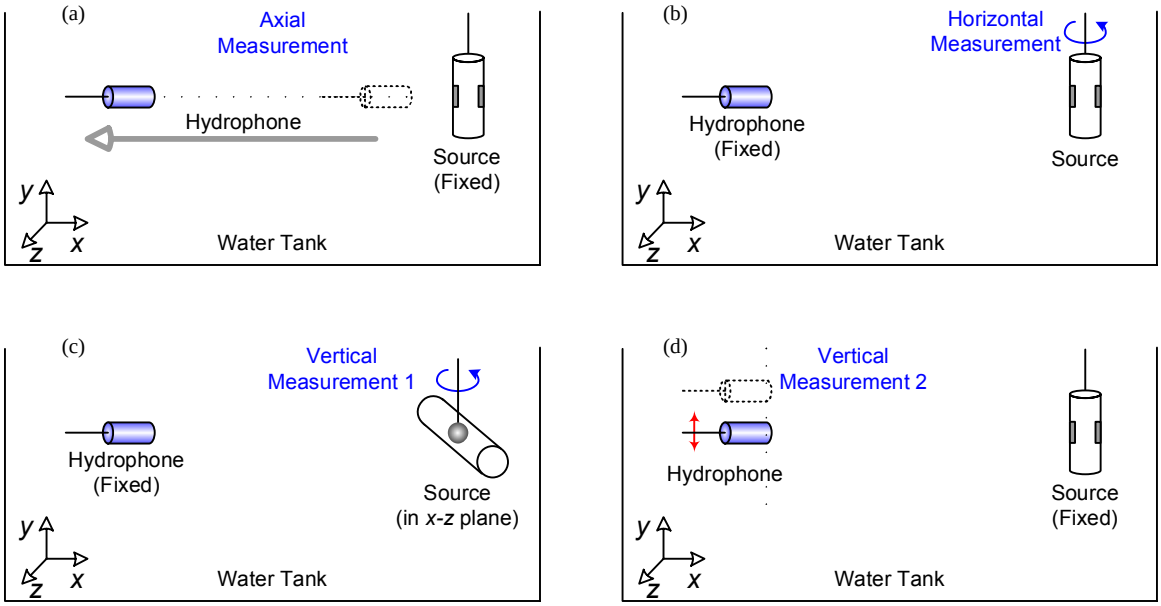

Figure 3 Schematic diagram of the experimental configurations in water measurement
(a) Axial measurement; (b) Horizontal measurement
(c) Vertical measurement 1; (d) Vertical measurement 2

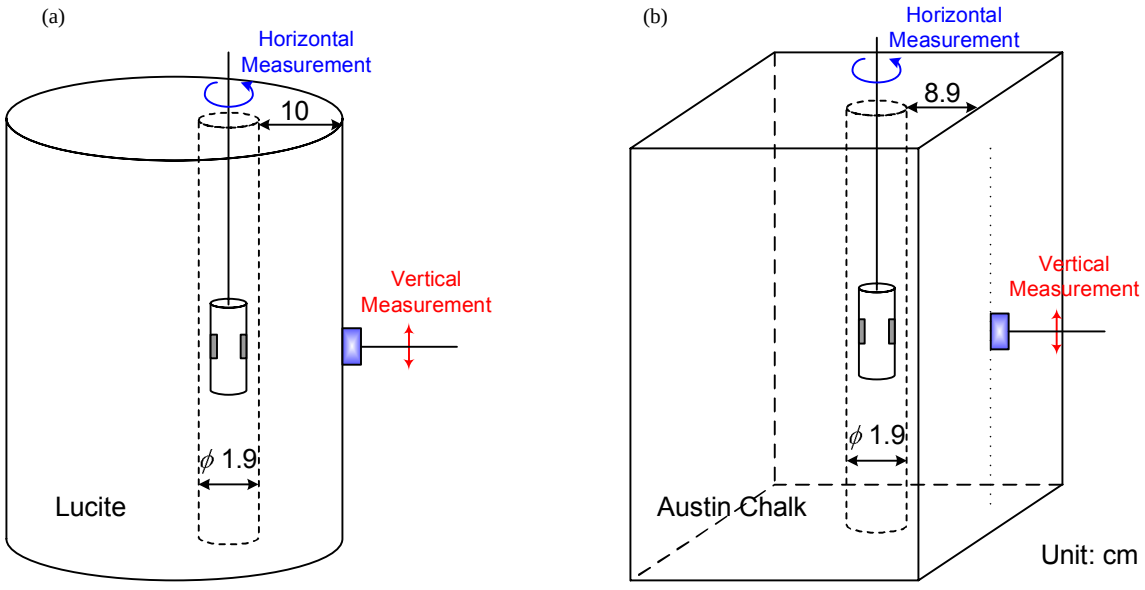

Figure 4 Schematic diagram of the experimental configurations in borehole measurements
(a) in Lucite block; (b) in Austin Chalk block

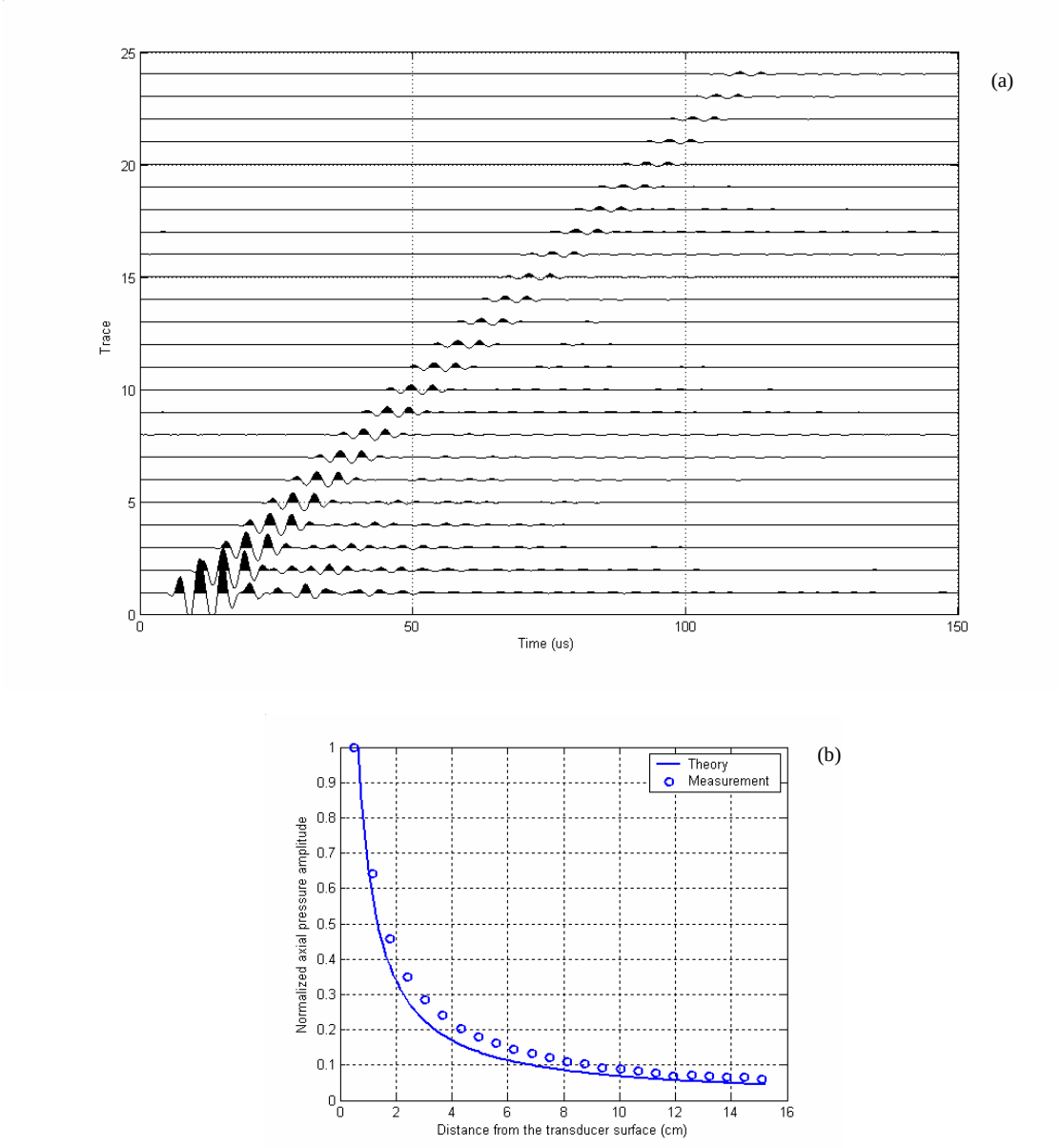

Figure 5 (a) Waveforms received at different distance
(b) the normalized axial pressure amplitude, numerical calculation and measurement data
Source frequency = 250KHz, Transducer radius = 3mm, $ka = \pi$

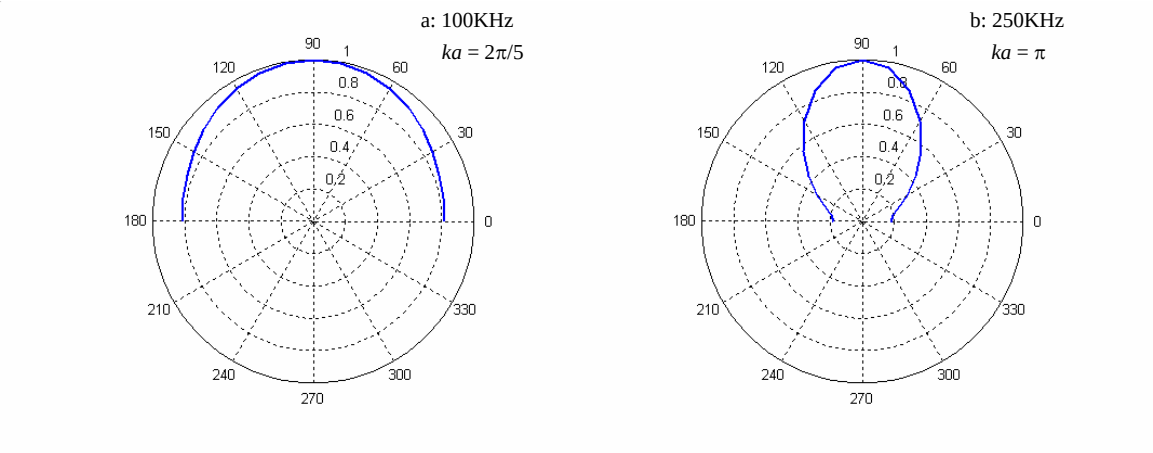

Figure 6 Theoretical horizontal radiation patterns for a piston transducer in an infinite baffle for different source frequencies

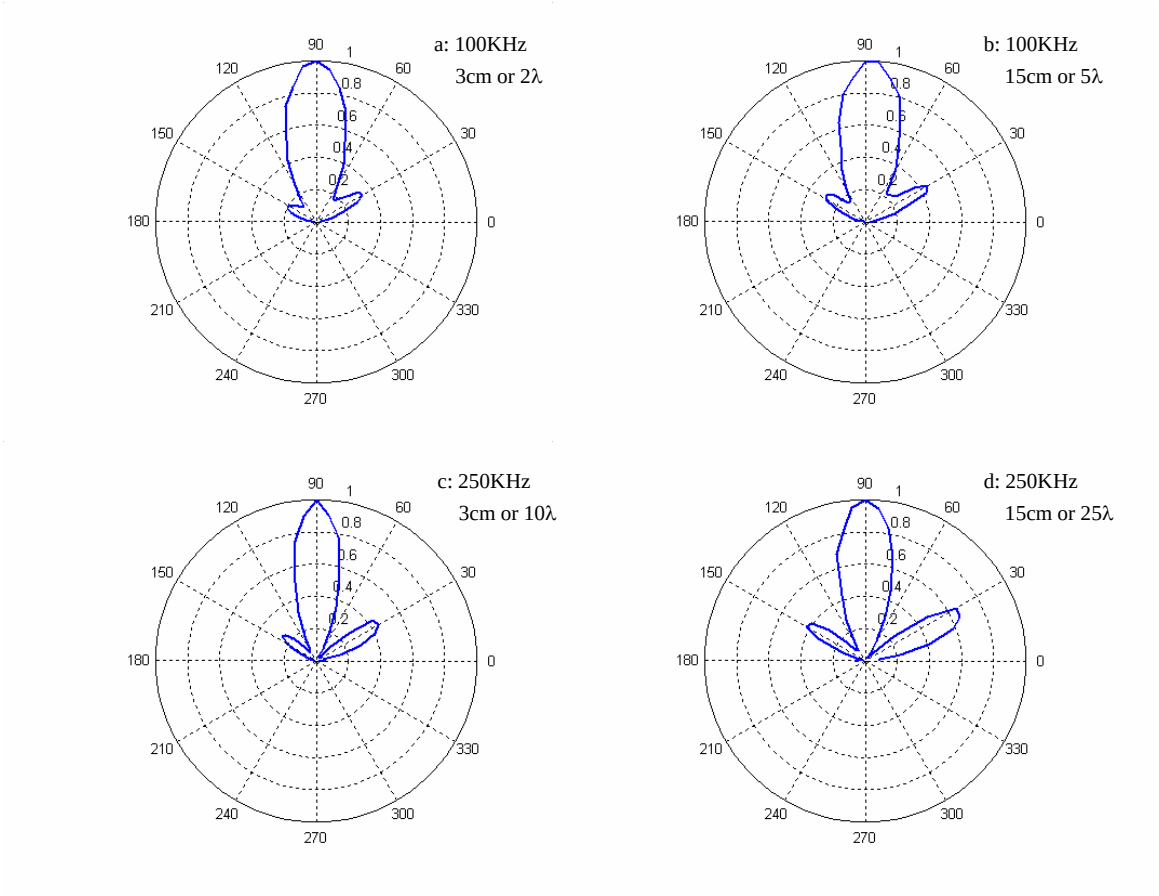

Figure 7 Horizontal radiation patterns in water for transducer in a small tool (10mm diameter) for different source frequencies and source-receiver separations

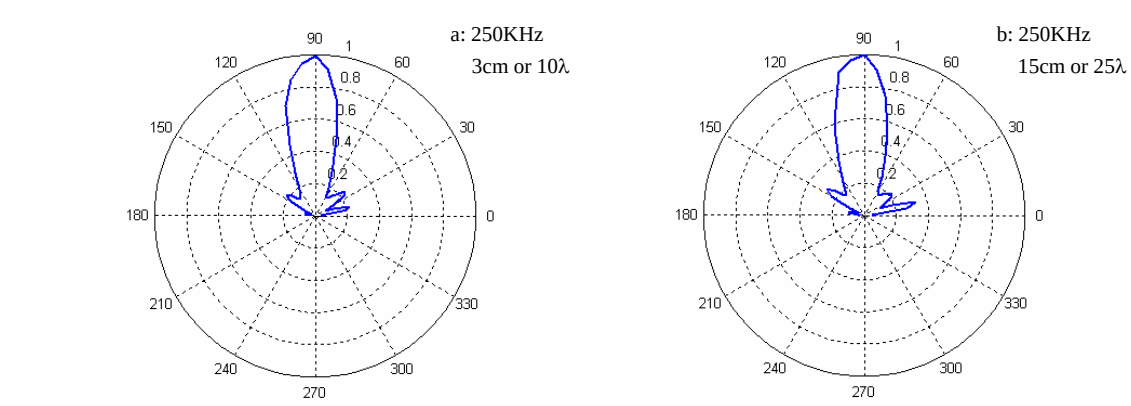

Figure 8 Horizontal radiation patterns in water for transducer in a larger tool (15mm diameter) for different source-receiver separations

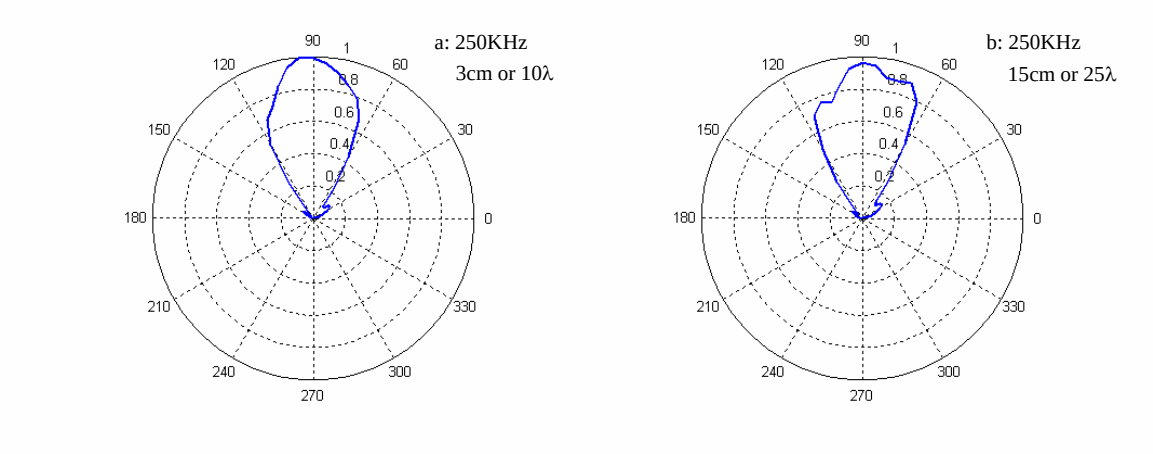

Figure 9 Vertical radiation patterns (method 1) in water for different source-receiver separations for small tool (10mm diameter)

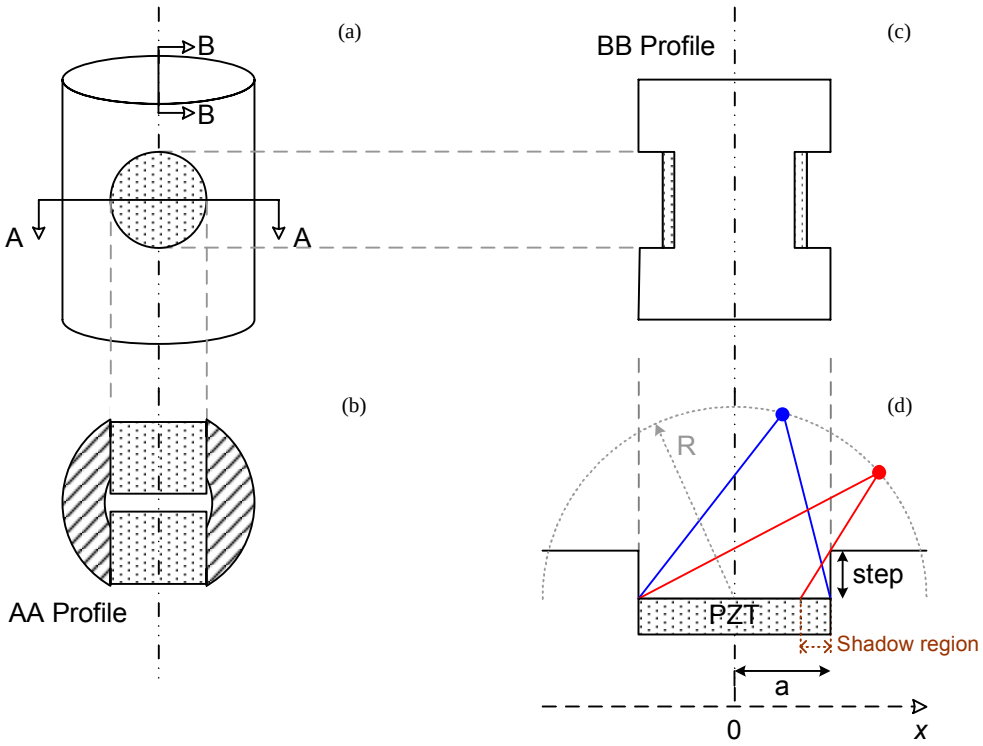

Figure 10 Approximate model for the source tool section

(a): source tool section shape

(b): vertical cross-section of the source tool section the longer axis

(c) horizontal cross-section of the source tool along the center of PZT plate

(d) one-dimensional simulation, a PZT plate inset in a steel tool

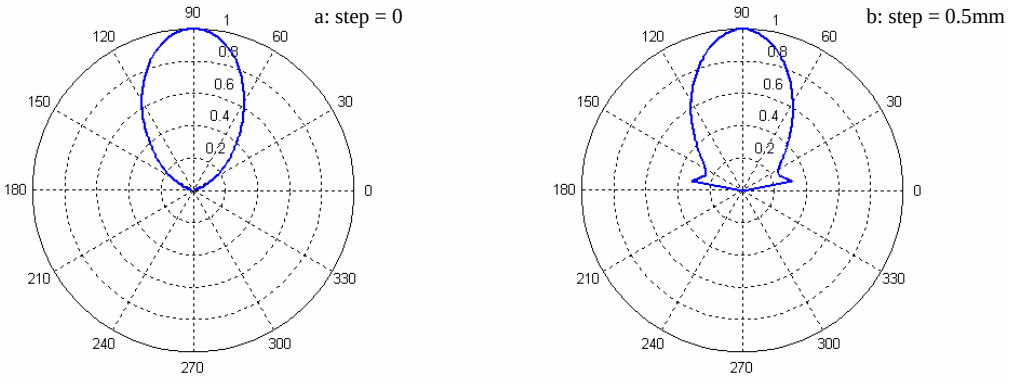

Figure 11 Theoretical calculation for the radiation pattern of the model shown in Figure 10(d)

(a): step = 0, i.e. the PZT plate in on the same level as the outer steel tool

(b): step = 0.5mm, i.e. the PZT plate in 0.5mm lower than the outer steel tool

Source frequency = 250KHz, Transducer radius = 3mm, $ka = \pi$

The inset is capable of introducing small side lobes.

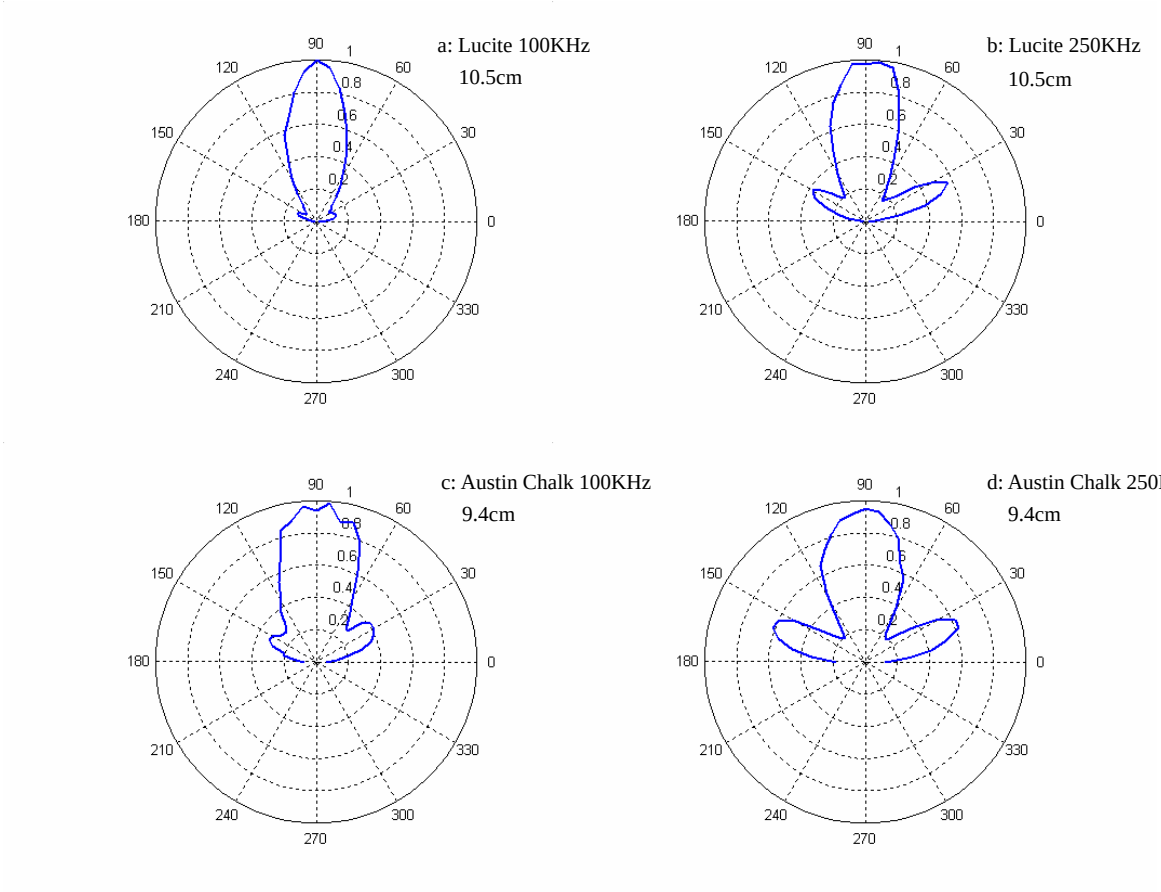

Figure 12 Horizontal compressional radiation patterns in borehole measurement
Lucite (a): 100KHz signal frequency, and (b): 250KHz signal frequency
Austin Chalk (c): 100KHz signal frequency, and (d): 250KHz signal frequency

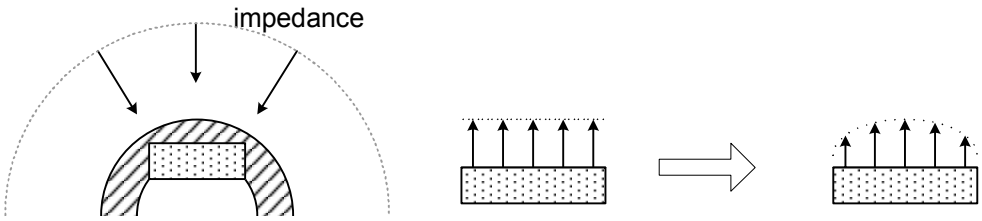

Figure 13 Approximate model for the borehole edge effect on transducer

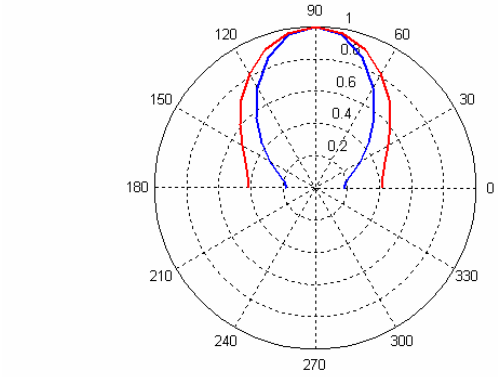

Figure 14 Numerical calculation for the effect of a curved impedance load on a piston transducer in an infinite baffle.

Source frequency = 250KHz, Transducer radius = 3mm, $ka = \pi$

blue line: homogenous impedance, no borehole situation

red line: curved impedance, borehole situation

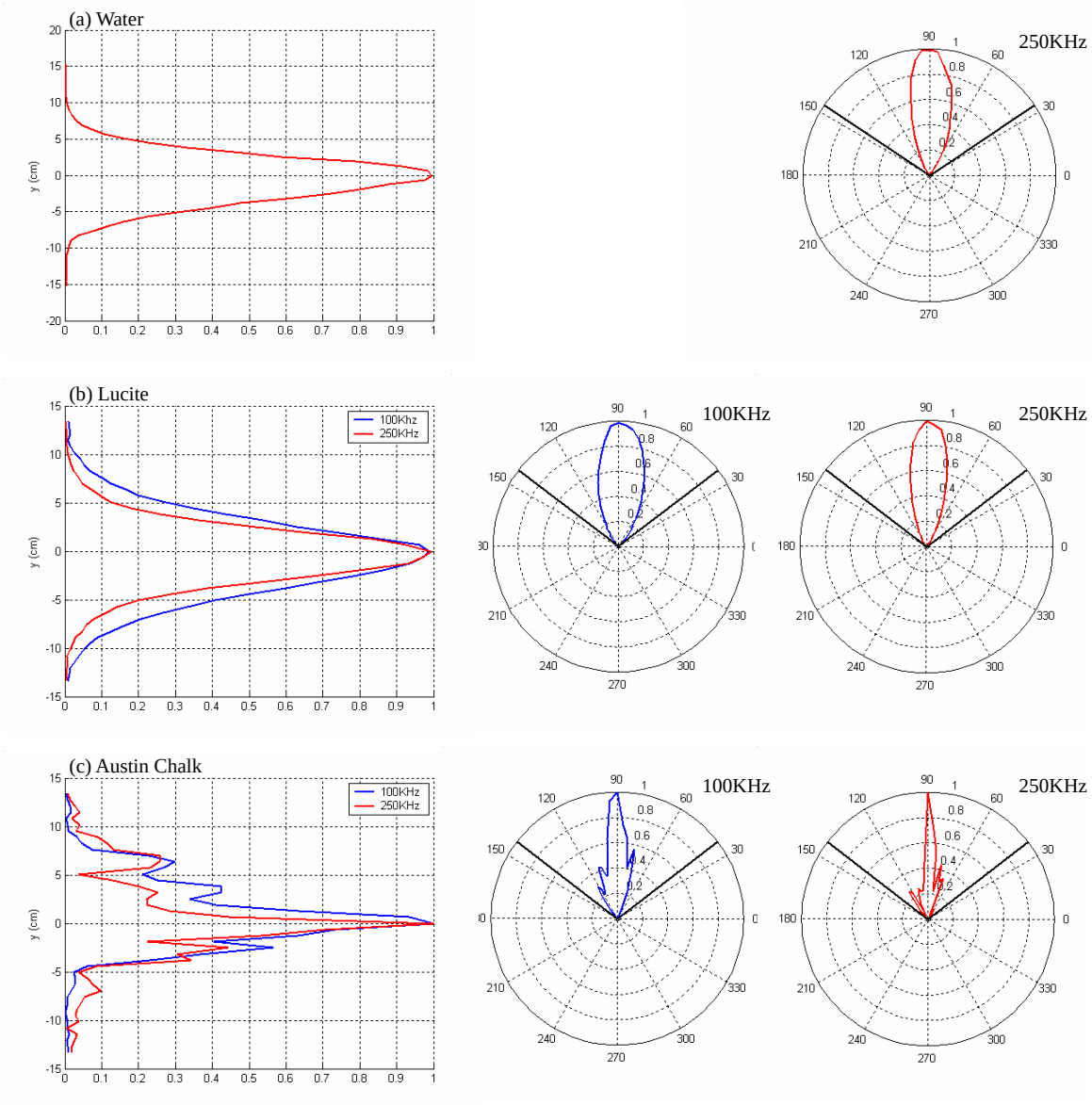

Figure 15 Vertical compressional radiation patterns in water and borehole measurements: (a) Water; (b) Lucite; (c) Austin Chalk